"High Dose Ion Implantation And Corrosion Behavior of Ferrous Metals"

B. D. Sartwell* and N. S. Wheeler
Bureau of Mines, 4900 LaSalle Road
Avondale, Md. 20782

G. K. Hubler and E. McCafferty
Naval Research Laboratory
Washington, D. C. 20375

C. R. Clayton
State University of New York
Stony Brook, New York 11794

There are two possible approaches to applying ion implantation to the modification of the corrosion behavior of metals and alloys. The first approach is to use ion implantation to produce metastable or amorphous corrosion-resistant surface alloys that are inaccessible by conventional metallurgical techniques, and to apply them to specific applications where corrosion is a severe problem. Secondly, and of a more fundamental nature, ion implantation can be used to introduce controlled amounts of various elements into the surface of a metal as part of a research effort to identify the mechanisms responsible for certain forms of general and localized corrosion. The technique of alloying to produce more corrosion resistant materials is widely used and the choice of a particular alloying element is usually based on the fact that it will enhance the formation of a passive film or will reduce the rate of the various cathodic processes that occur on the metal's surface. It is also possible to

reduce the overall corrosion rate by introducing an element that displays rapid cathodic kinetics, but it is essential that the original material passivate in the corrosive environment that is being considered.

Aqueous corrosion proceeds through an electrochemical mechanism and there are various types of electrochemical techniques used to evaluate the corrosion resistance of alloys. Linear polarization and Tafel region extrapolation have been used to evaluate binary Fe-Pb and Fe-Ti surface alloys formed by ion implantation. The instantaneous corrosion rate of the Fe-Pb alloys in 0.1 $\underline{N}$ H_2SO_4 was approximately 3 to 4 times lower than that of pure iron. The reason for this is a decrease in the hydrogen exchange current density caused by the presence of the lead, which is a poison for the hydrogen evolution reaction. The corrosion rate of the Fe-Ti alloys was approximately two times higher than that of iron. Auger analysis of the Fe-Ti alloy before exposure to the acid solution indicated that TiC was in the region about 4.5 to 34 nm from the surface. SEM analysis following the electrochemical tests revealed the presence of square flat-bottomed pits, a morphology which is usually associated with inclusion etch pits. Thus, it is proposed that the square pits may have been formed as TiC precipitates were etched from the sample surface.

The implantation of zirconium into iron reduces the corrosion rate by an order of magnitude by enhancing the rate of passivation in a 1 $\underline{N}$ H_2SO_4 solution. The corrosion rate is still considerably higher, however, than that observed for an

amorphous $Fe_{90}Zr_{10}$ coating even though the near-surface concentration of Zr in the implanted sample was estimated to be 20 to 30 atomic percent.

The implantation of Ti into 52100 steel results in the formation of an amorphous Ti-Fe-C surface, which provides modest improvements in corrosion resistance in 1 N H_2SO_4 and 0.1 N NaCl. The anodic current density in both solutions is about 10% that of unimplanted 52100 steel, up to an anodic overpotential of about 800 mV. Pitting, which is initiated at low overpotentials, leads to undermining of the implanted layer and its eventual peeling off at higher potentials. Detailed optical and surface analytical studies show that the pitting initiates at surface flaws, which are most likely surface carbides or oxide inclusions. Galvanic action between free Ti beneath the pitted amorphous film and Fe in the bulk steel thus leads to undermining of the amorphous layer.

The effect of the implantation of various ions on the pitting corrosion resistance of 52100 steel in a 0.01M NaCl solution has been investigated. Molybdenum implantation provided very little improvements; however, a combination of both chromium and molybdenum significantly increased the breakdown potential for initiation of pitting corrosion. Finally, tantalum implantation proved to be the most effective in protecting the surface of the 52100 from pitting corrosion.

---

*Present Address: Naval Research Laboratory, Code 6675, Washington, D.C. 20375

TABLE 1. - Corrosion rates, expressed in mils/year, in 0.1 N H_2SO_4 for several different metals and ion-implanted allovs using two different test methods, Tafel extrapolation and three-point linear polarization

Test method	Fe	Fe-Pb	Pb	Fe-Ti	Ti
Tafel extrapolation..	50±2	12±2	0.42±0.19	96±22	0.69±0.04
Linear polarization...	32±9	16±10	(1)	55±47	0.98±0.52

[1]Could not measure corrosion rate due to cathodic Tafel slope being indeterminate.

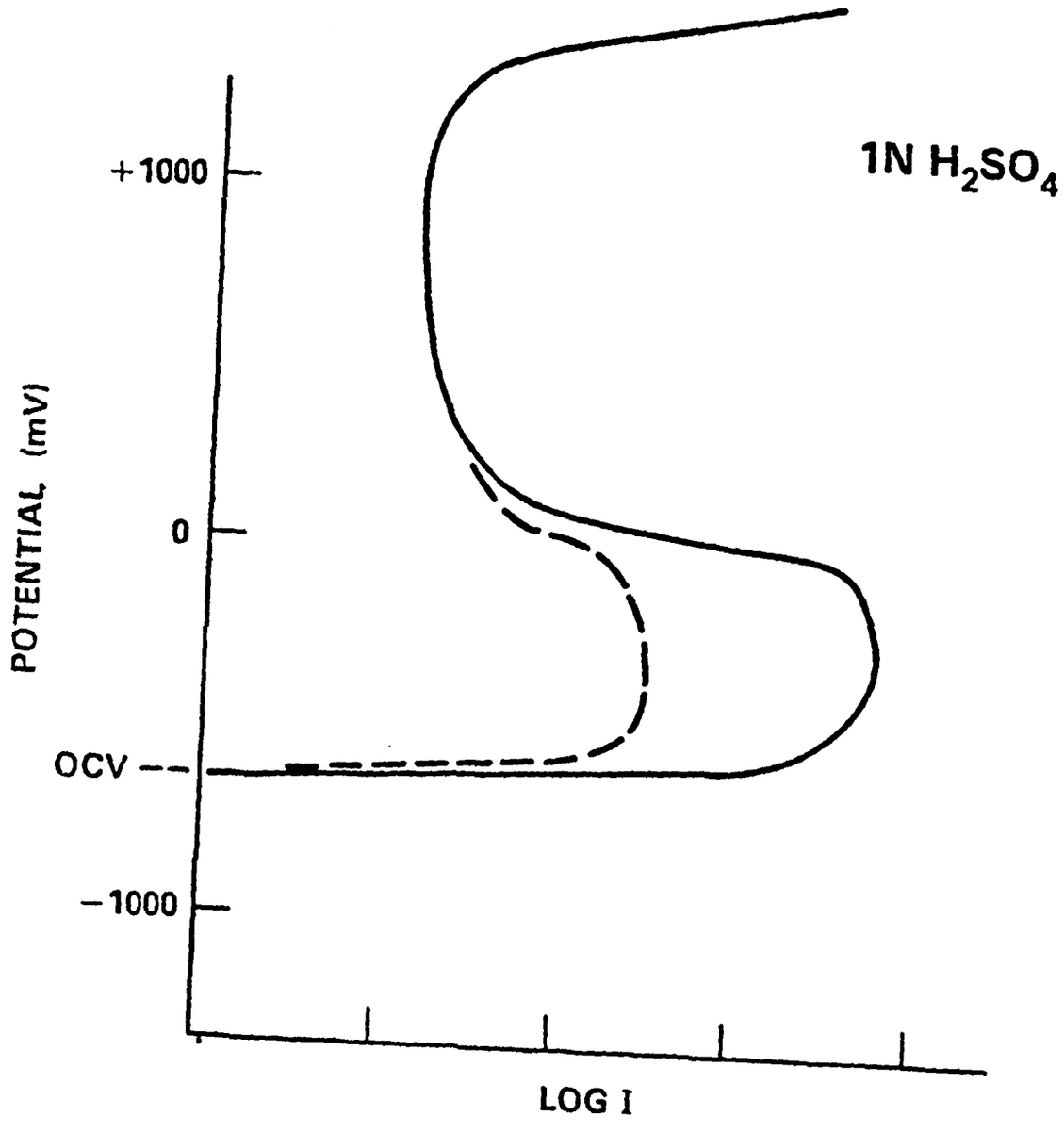

FIGURE 1. Idealized potentiodynamic polarization scan (current vs. voltage characteristic) for a ferrous alloy in 1N H_2SO_4 at room temperature. The dashed line indicates an improvement in the passivity of the surface and therefore improved corrosion resistance.

FIGURE 2

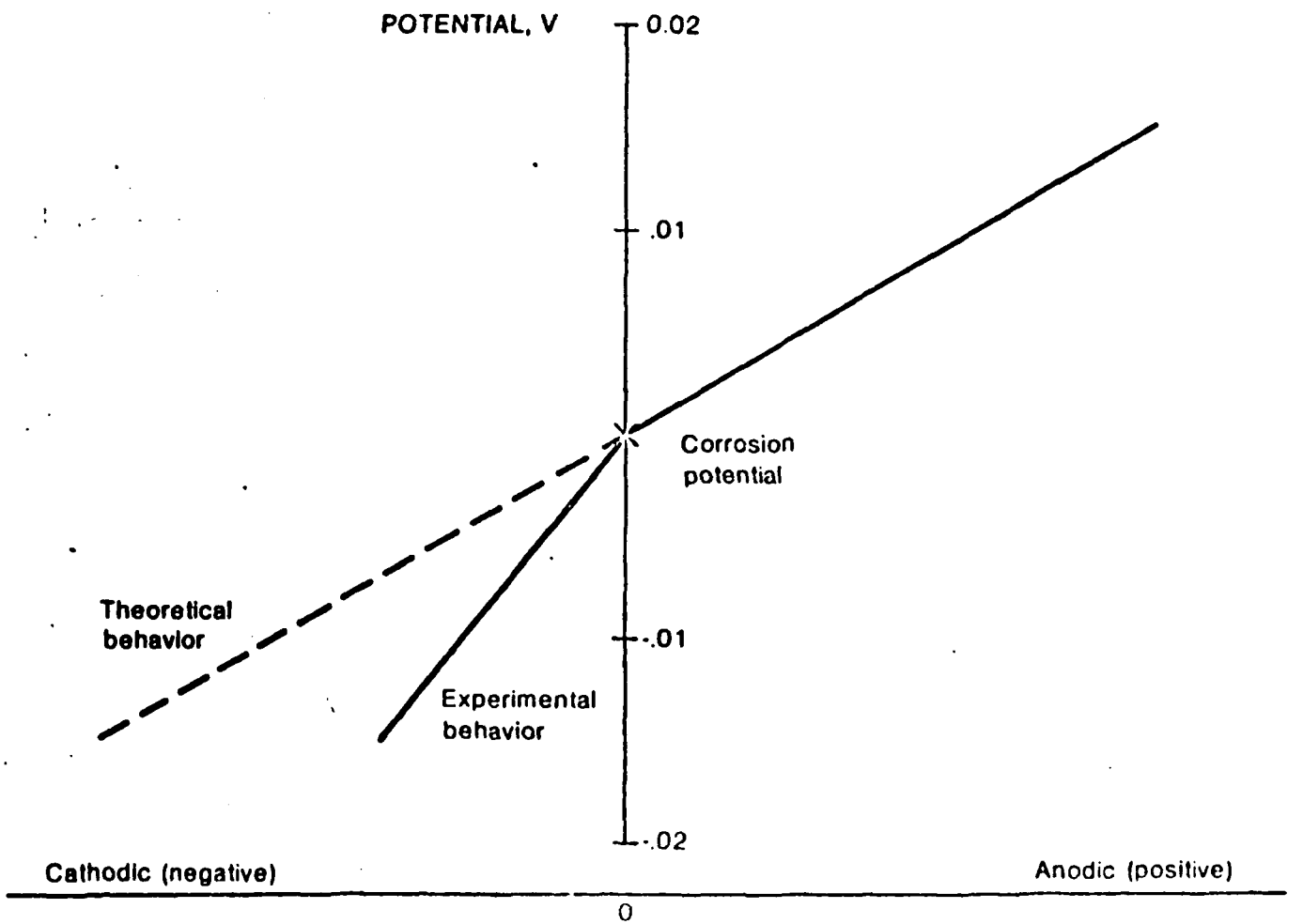
POTENTIAL, V
0.02
.01
-.01
-.02
Corrosion potential
Theoretical behavior
Experimental behavior
Cathodic (negative)
Anodic (positive)
0

Figure Caption

FIGURE 2 . Two electrochemical methods used for determining corrosion rates were Tafel region extrapolation and three-point linear polarization. The former determines the corrosion rate graphically whereas the latter requires calculations based on experimental data. When the logarithm of the absolute value of the measured current density is plotted against the sample potential, the resulting curve generally has two linear portions (Tafel regions), one on the anodic and one on the cathodic side of the SOOC (steady-state open-circuit) potential. Extrapolation of the Tafel regions gives a point of intersection, the coordinates of which are the corrosion potential E_c and the corrosion current density I_c, or corrosion rate.

The basis for linear polarization, or polarization resistance, lies in the assumption that potential varies linearly with current density for a range of ± 20 mV from E_c, as illustrated in this figure. The slope of this line can be related to the Tafel region slopes (found from log I vs. E curves) to give I_c. Some metal/environment systems display linear E vs. I curves, but most are nonlinear as shown by the solid line. The three-point linear polarization method was devised to provide a means for determining the slope of the E vs. I curve in the nonlinear case.

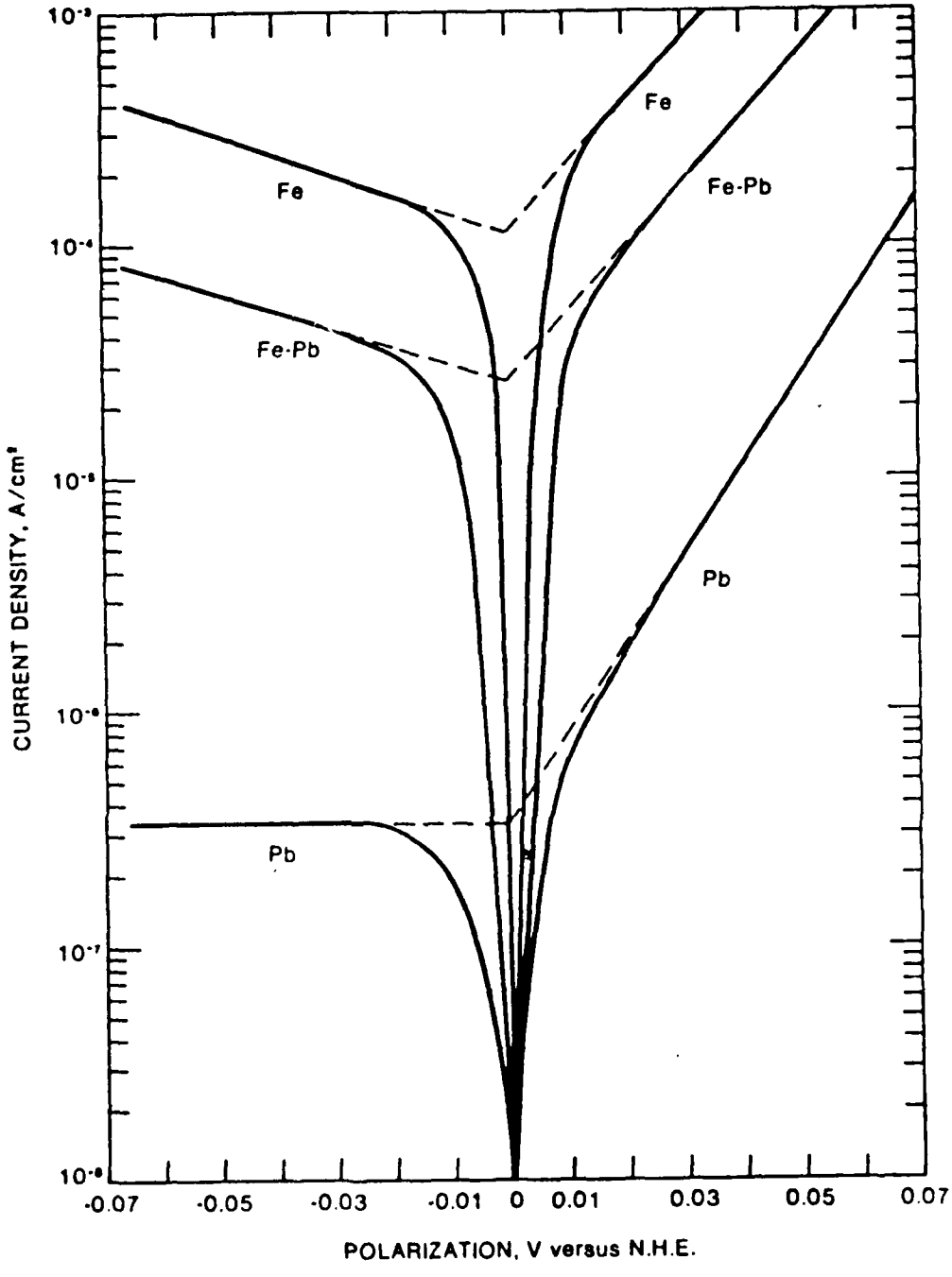

FIGURE 3. Current density as a function of sample potential for Fe, Pb, and Fe implanted with 30 keV Pb^+ such that the final retained dose was 1.6×10^{16} atoms/cm^2. The potential is shown as volts from the steady-state open-circuit potential. The dashed lines represent the extrapolation from the Tafel region of each curve.

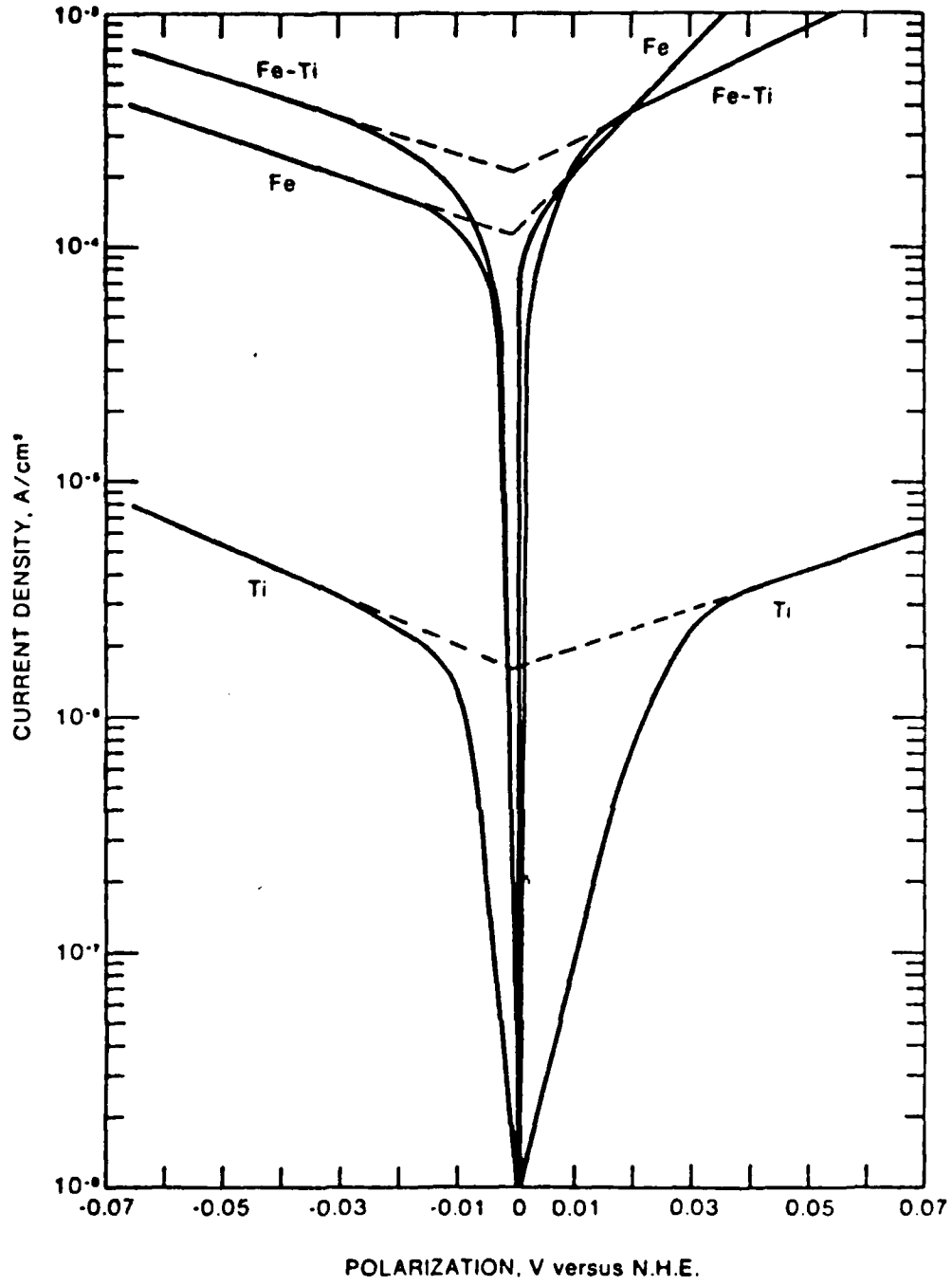

FIGURE 4 . Current density as a function of sample potential for Fe, Ti, and Fe implanted with 50 keV Ti^+ to a total retained dose of 7×10^{16} atoms/cm^2, with the potential shown as volts from the SSOC potential.

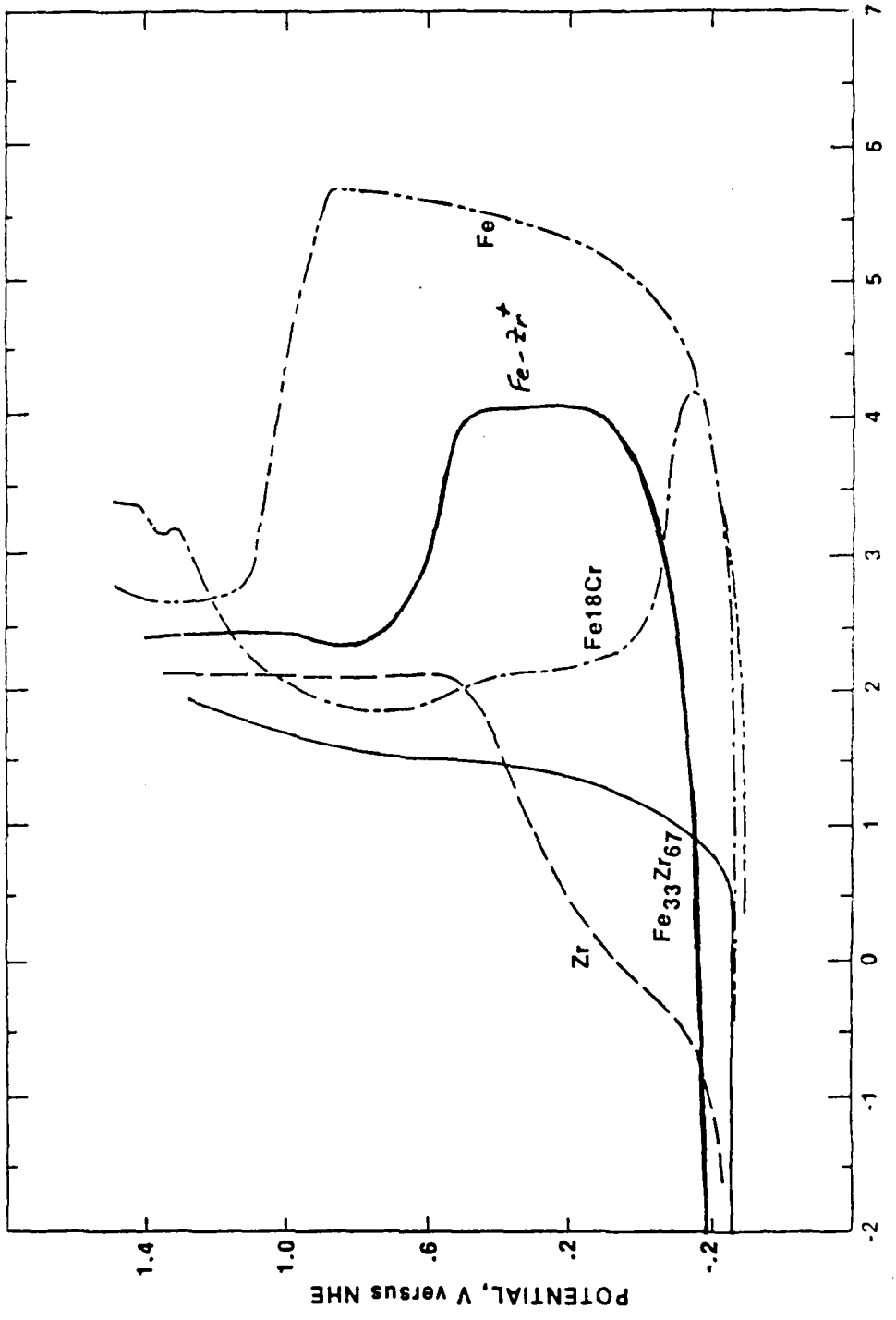

FIGURE 5. Polarization curves in deaerated 1N H_2SO_4 obtained at a rate of 60 V/hour for Fe, Fe-18Cr, Zr, an $Fe_{33}Zr_{67}$ amorphous coating, and Fe implanted with 150 keV Zr^+ to a dose of 2 x 10^{17} ions/cm².

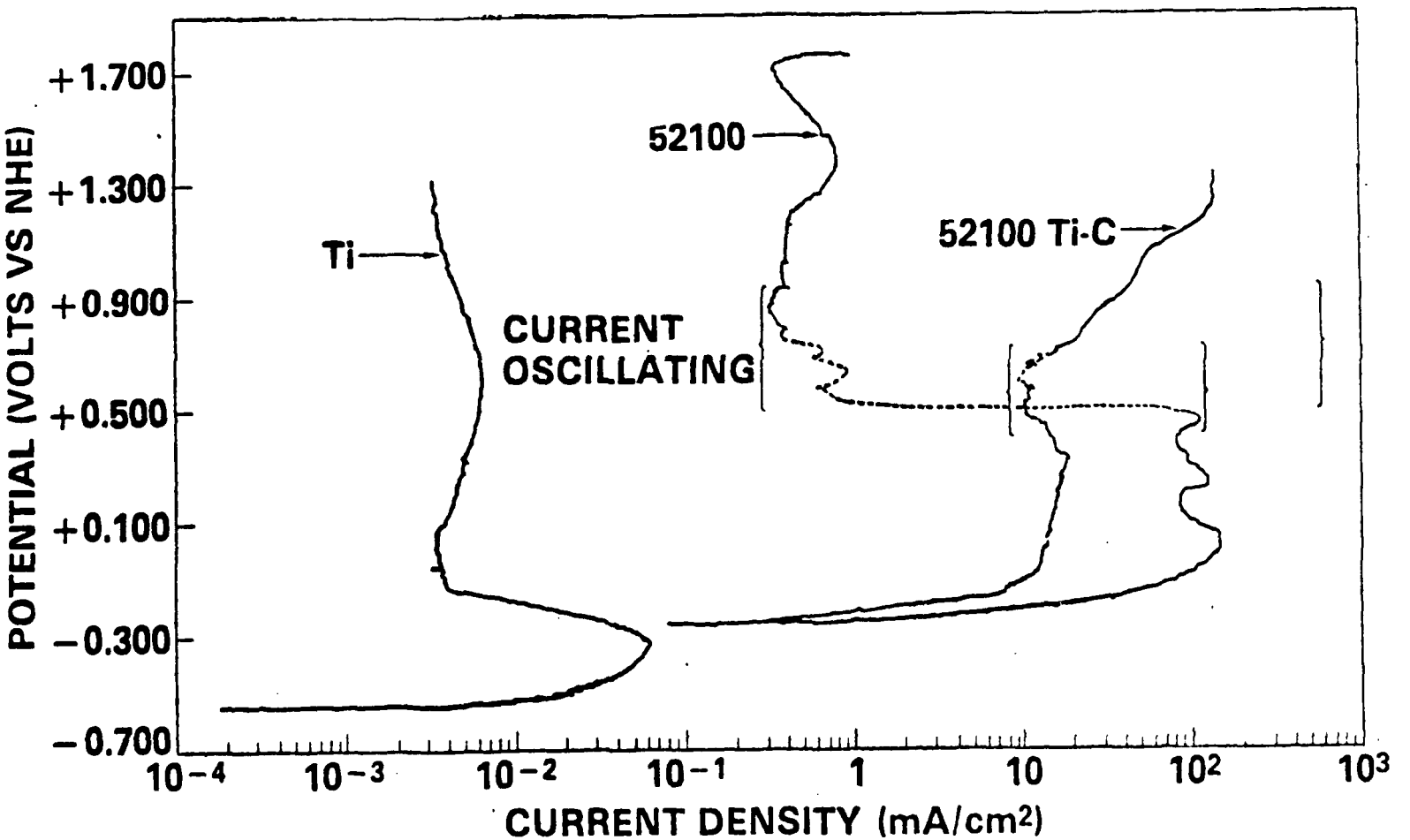

FIGURE 6 . Anodic potentiodynamic polarization curves (10 mV/min) for pure Ti, 52100 steel, and Ti-implanted 52100 steel (4.6×10^{17} ions/cm², 190 keV) in deaerated 1N H_2SO_4.

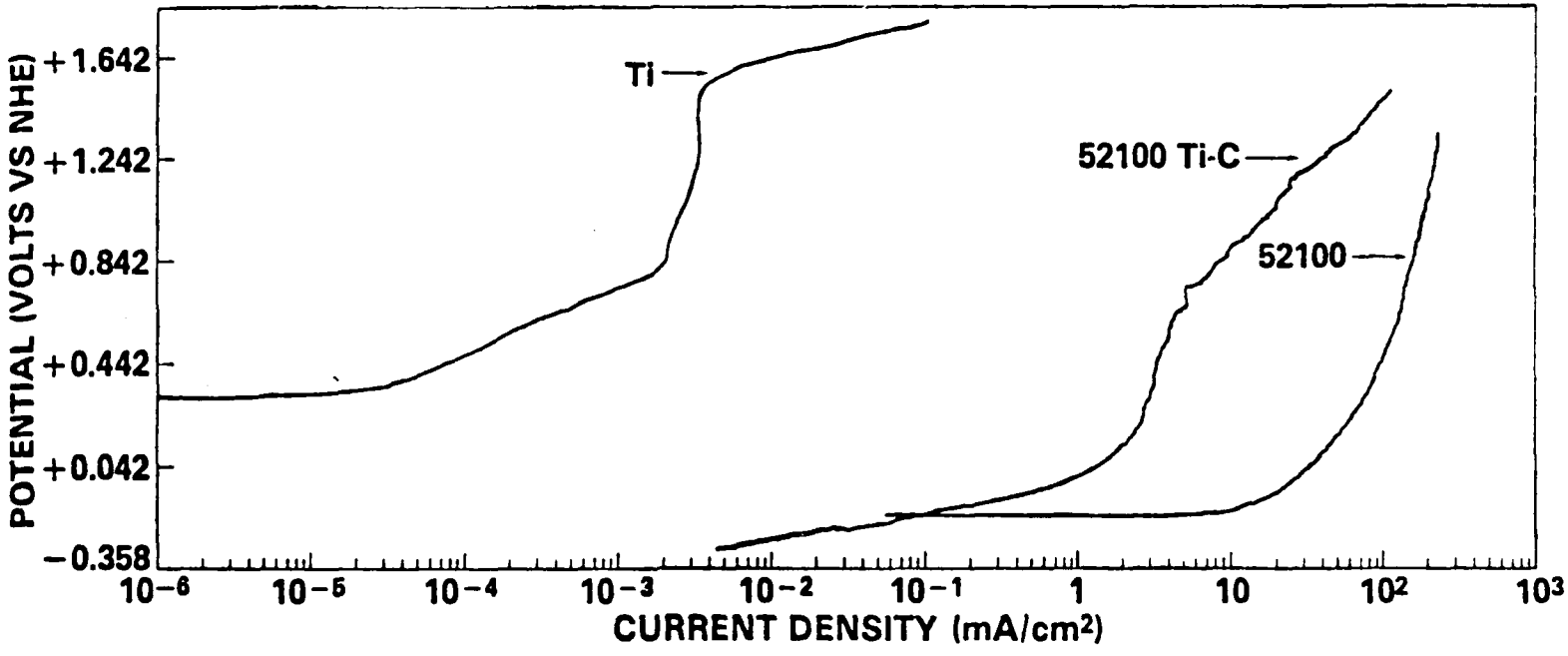

FIGURE 7 . Anodic potentiodynamic polarization curves for unimplanted 52100 steel and Ti-implanted 52100 steel (4.0×10^{17} ions/cm^2 at 190 keV) in 0.1 M NaCl solution.

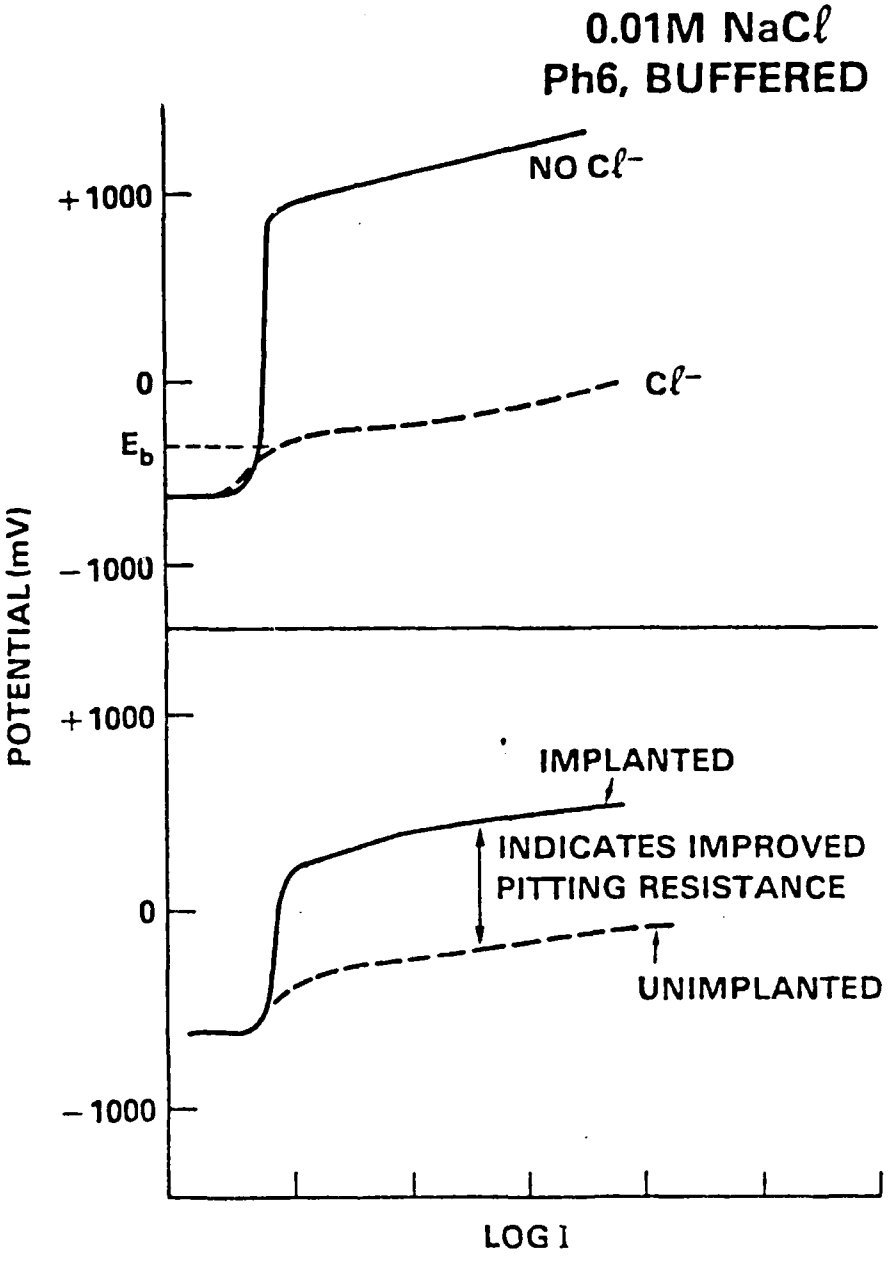

FIGURE 8. Idealized potentiodynamic polarization scans (current vs. voltage characteristic) for a ferrous alloy in a buffered pH 6 solution at room temperature. The upper set of curves demonstrate the effect of adding Cl^- ions to the solution. E_b defines the pitting potential where a sharp increase in current results when pits form on the surface. The lower set of curves demonstrate the desired result of ion implantation, i.e., force the pitting potential toward higher values.

FIGURE 9 . Potentiodynamic anodic polarization data produced in buffer solution of pH6 containing 0.01M NaCl for 52100 steel, and for 52100 steel implanted with molybdenum (3.5×10^{16} ions/cm^2), chromium (2×10^{17} ions/cm^2 at 150 keV), chromium plus molybdenum (2×10^{17} Cr/cm^2 at 150 keV, 3.5×10^{16} Mo/cm^2 at 100 keV), and tantalum (1×10^{17} ions/cm^2 at 150 keV). The curves indicate that tantalum was most effective in protecting the surface from pitting corrosion.